Kinetic and Structural Studies of Specific Protein−Protein Interactions in Substrate Catalysis by Cdc25B Phosphatase†

Jungsan Sohn,‡ Gregory Buhrman,§ and Johannes Rudolph*

Departments of Biochemistry and Chemistry, Duke University Medical Center, Durham, North Carolina 27710

Received June 23, 2006; Revised Manuscript Received October 17, 2006

ABSTRACT: Using a combination of steady-state and single-turnover kinetics, we probe substrate association, dissociation, and chemistry for the reaction of Cdc25B phosphatase with its Cdk2-pTpY/CycA protein substrate. The rate constant for substrate association for the wild-type enzyme is 1.3×10^6 M^{-1} s^{-1}. The rate constant for dissociation is slow compared to the rate constant for phosphate transfer to form the phospho-enzyme intermediate ($k_2 = 1.1$ s^{-1}), making Cdk2-pTpY/CycA a sticky substrate. Compared to the wild type, all hotspot mutants of residues at the remote docking site that specifically affect catalysis with the protein substrate (Arg488, Arg492, and Tyr497 on Cdc25B and Asp206 on Cdk2) have greatly slowed rate constants of association (70- to 4500-fold), and some mutants have decreased k_2 values compared to that of the wild type. Most dramatically, R492L, despite showing no significant changes in a crystal structure at 2.0 Å resolution, has an ~100-fold decrease in k_2 compared to that of wild-type Cdc25B. The active site C473S mutant binds tightly to and dissociates slowly from Cdk2-pTpY/CycA ($K_d = 10$ nM, $k_{off} = 0.01$ s^{-1}). In contrast, the C473D mutant, despite showing only localized perturbations in the active site at 1.6 Å resolution, has a much weaker affinity and dissociates rapidly (K_d of 2 μM, $k_{off} > 2$ s^{-1}) from the protein substrate. Overall, we demonstrate that the association of Cdc25B with its Cdk2-pTpY/CycA substrate is governed to a significant extent by the interactions of the remote hotspot residues, whereas dissociation is governed by interactions at the active site.

Protein−protein association is one of the most intriguing and important biochemical events, especially when considered in the context of the living cell. How intracellular proteins are able to specifically and rapidly associate and dissociate to create the necessary regulatory pathways that govern life processes is not well understood. This problem appears to be particularly complex for protein-modifying enzymes such as protein kinases and protein phosphatases. There exist >500 protein kinases and >150 protein phosphatases in the human cell. These enzymes modify the sidechains of only three amino acids (Ser, Thr, and Tyr). Yet for well-ordered signal transduction pathways to exist without cross-talk, these protein kinases and phosphatases must exhibit specificity toward their correct physiological substrates. Unlike the paradigm from proteases (e.g., trypsin cleaving after Arg or Lys), the specificity for protein kinases and phosphatases is mediated only in part by the primary amino acid sequence adjacent to the site of phosphorylation. Docking sites often located remote from the sites of phosphorylation and dephosphorylation can play a major role in substrate selectivity. Although protein docking sites typically encompass extensive protein−protein interfaces, only 5−10% of the residues at these interfaces, so-called hotspot residues, contribute significantly to the energetics of binding (*1*, *2*). The mechanistic roles of hotspot residues have been dissected for a few high affinity protein−protein complexes, such as antibody−antigen complexes (*3*, *4*), RNases with their protein inhibitors (*5*), and TEM1β lactamase with its protein inhibitor (*6*). For the more transient and weaker protein−protein interactions that occur for protein-modifying enzymes, such as protein kinases and phosphatases, the mechanisms by which hotspot residues contribute to substrate recognition and subsequent chemistry at the distant active site is rarely studied and, thus, poorly understood. How one such protein-modifying enzyme, the Cdc25B phosphatase, recognizes its protein substrate, the Cdk2-pTpY/CycA[1] complex, via its active site and a remote docking site is the subject of this publication. Because this protein−protein interaction involves an enzymatic reaction, we take advantage of the rich methodology of enzymology.

Cdc25 phosphatases are important regulators of the cyclin-dependent kinases, the main gatekeepers of the eukaryotic cell division cycle (*7*, *8*). Specifically, the Cdc25s trigger the final activation of these complexes by removing two inhibitory phosphates near the active sites of the kinase subunits (pThr14, pTyr15 in Cdk2 numbering). Of the three human Cdc25s, Cdc25A controls both the G1/S and G2/M transitions, whereas Cdc25B and Cdc25C are regulators of G2/M. Given their significant involvement in cell cycle

† This work was supported by NIH Grant R01 GM61822.

* To whom correspondence should be addressed. Phone: (919) 668-6188. Fax: (919) 613-8642. E-mail: rudolph@biochem.duke.edu.

‡ Current address: Department of Biology, MIT Cambridge, MA 02139.

§ Current address: Department of Biochemistry, North Carolina State University, Raleigh, NC 27695.

[1] Abbreviations: Cdk2-pTpY/CycA, cyclin-dependent kinase 2 complexed with cyclin A and bis-phosphorylated on Thr14 and Tyr15; PTP, protein tyrosine phosphatase; RMSD, root mean square deviation; E•S, enzyme−substrate; CD, common docking.

10.1021/bi061257y CCC: $37.00
Published on Web 12/22/2006

control, it is not surprising that the Cdc25s are closely linked to oncogenesis (*9*) and the cellular response to DNA damage (*10*). The overexpression of Cdc25A and/or Cdc25B, but not Cdc25C, is observed in numerous cancers and is often correlated with a poor clinical prognosis. Thus, Cdc25 phosphatases have been of interest as anticancer targets in both academia and industry.

Cdc25 phosphatases belong to the family of dual-specificity phosphatases, a subfamily of the protein tyrosine phosphatases (PTPs) (*11*). Although the Cdc25 phosphatases show no significant overall sequence or structural homology to the PTPs, they do contain the conserved catalytic motif common to all PTPs. In this motif, C is the catalytic cysteine, and the amide backbones of the five X residues form a phosphate-binding loop along with the arginine R. The structure of this active site loop is identical in all known PTPs. Substrate selection by the PTPs is a particularly vexing problem because most of these phosphatases are small globular domains with no obvious recognition sites for substrates. Although some of these phosphatases (e.g., PTP1b) have an active site pocket that accommodates at least a pTyr residue, there exists no adjacent region that can be readily identified as a peptide-binding site. Others, including the Cdc25s in particular (*12*, *13*), instead have an active site that is solvent exposed, and protein substrate recognition appears only possible via a broad protein−protein interaction. In accord with this conjecture, Cdc25 phosphatases display a 10^6-fold preference for protein substrate vs peptidic substrates that mimic the target dephosphorylation site (*14*). Also, Cdc25s utilize a remote docking site >20 Å from the active site that is specifically involved in the recognition of the protein substrate (*15*, *16*).

The enzymatic reaction mechanism of the Cdc25 phosphatases, like those for most other protein-modifying enzymes, has been primarily characterized using artificial substrates (*17*−*20*). Our prior studies using the protein substrate Cdk2-pTpY/CycA have relied mostly on steady-state kinetics. For example, the dramatic preference for protein substrate versus peptidic substrates was determined using the specificity constant (k_{cat}/K_m). We have also used k_{cat}/K_m measurements to identify, characterize, and measure interaction energies for three hotspot residues on Cdc25B (Arg488, Arg492, and Tyr 497) and one hotspot residue on Cdk2 (Asp206) that decrease catalysis by up to 600-fold while not affecting the activity toward small molecule substrates (*15*, *16*). As commonly acknowledged (*21*), steady-state kinetics alone do not reveal microscopic rate constants and, thus, shed limited insight into detailed reaction mechanisms. We, therefore, use herein a combination of steady-state and single-turnover kinetics to probe the kinetics of substrate association, dissociation, and chemistry for the reaction of Cdc25B phosphatase with its Cdk2-pTpY/CycA protein substrate. We complement our kinetic analysis with structural studies of two Cdc25B mutants, namely, the hotspot mutant R492L and the active site mutant C473D.

MATERIALS AND METHODS

Protein Expression, Purification, and Crystallography. The catalytic domain of Cdc25B, the hotspot mutants, and the active site mutants C473S and C473D were expressed as untagged proteins in *E. coli* as described (*15*, *18*). The crystal structures of Cdc25B(R492L) and Cdc25B(C473D) were determined as previously described for the wild type (*22*) and the C473S mutant (*16*), and the coordinates have been deposited in the PDB (PDB codes 2IFD and 2IFV, respectively). The Cdk2/CycA complex in which CycA is truncated and encompasses residues 174−432 was prepared as previously described (*23*). The soluble domain of the dual-specificity kinase Myt1 was expressed as a GST-tagged protein in *E. coli* (*24*) and purified as described (*14*). The bis-phosphorylated Cdk2-pTpY/CycA substrate was prepared fresh daily by incubation of Cdk2/CycA with GST-Myt1 bound to glutathione-Sepharose beads and 2.5 mM [γ-^{32}P]-ATP (200-500Ci/mol) for 2.5 h at RT. Remaining ATP and GST-Myt1 were removed by G-50 chromatography.

Steady-State Kinetics. All phosphatase reactions were performed in a three-component (3C) buffer (50 mM Tris, 50 mM Bis-Tris, and 100 mM Na acetate at pH 6.0−6.5) containing 2 mM dithiothreitol at 25 °C. The activity of Cdc25B with Cdk2-pTpY/CycA was assayed by monitoring the release of inorganic phosphate from pThr14. Reactions were initiated by the enzyme (or substrate for the competitive binding assays) in the presence of 1 mg/mL BSA and 0.05% Tween 20 and quenched and precipitated by adding 3−5 volumes of 30% trichloroacetic acid (TCA). After centrifugation at 4 °C at 14 000*g* for 20 min or 2000*g* for 2 h for assays in 96-well plates to remove the unreacted substrate, the supernatant was subjected to scintillation counting. For k_{cat}/K_m measurements under initial velocity conditions, time dependence (5 points minimum), substrate concentration dependence (2−3 differing concentrations), and enzyme concentration dependence (3−4 differing concentrations) were tested to ensure adherence to Michaelis−Menten conditions.

Transient Kinetics. All single-turnover assays were performed using at minimum a 5-fold excess of the enzyme Cdc25B over the substrate Cdk2-pTpY/CycA. Single-turnover experiments at 5−120 s were performed using manual quench time points. All manual quench single-turnover reactions were stopped with 30% TCA, and the formation of inorganic phosphate was quantitated as described for the k_{cat}/K_m measurements. For single-turnover experiments at 5−3000 ms, rapid quench flow (RQF-400, Bio-Logic) was used. Reactions were initially quenched at each time point with 2 M HCl. An equal volume of 30% TCA was subsequently added to precipitate all of the proteins, and the released phosphate was quantitated as described for the steady-state measurements. At least two different substrate concentrations and four different enzyme concentrations were used to verify adherence to single-turnover conditions.

C473S, C473D, and Cdk2/CycA Binding Kinetics. The association of C473S to Cdk2-pTpY/CycA was monitored by measuring the time-dependent depletion of substrate available to react with wild-type Cdc25B. C473S (75−150 nM) was mixed with 20 nM protein substrate. At each time point, aliquots were transferred into a reaction vessel containing 1/15 volume of wild-type Cdc25B (3 μM final). After incubation for 5 s (timing by metronome) in order to completely remove the phosphate from the unbound substrate, the reaction was quenched by the addition of 3× the volume of 30% TCA. Insignificant dissociation of C473S from Cdk2-pTpY/CycA occurred during this 5 s incubation.

Scheme 1: Kinetic Model for the Catalytic Reaction Performed by Cdc25B

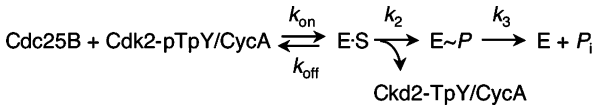

The dissociation of C473S from Cdk2-pTpY/CycA was monitored by measuring the time-dependent increase in the substrate available to react with wild-type Cdc25B. Cdk2-pTpY/CycA (50−80 nM) was preincubated with a slight excess of C473S (200−300 nM) for 5 min to form a complex. Excess wild-type Cdc25B (8−20 μM final) was then added, and aliquots were taken at each time point and quenched with 30% TCA. In a similar fashion, we attempted to measure the dissociation of C473D from Cdk2-pTpY/CycA. Preincubation of 30 μM C473D (15 × K_i) with 120 nM Cdk2-pTpY/CycA for 10 min was followed by the addition of wild-type Cdc25B. Aliquots at each time point (first point = 5 s) were quenched with 30% TCA.

Biacore Experiments. The NTA chip was charged with nickel and regenerated between each run according to the manufacturer's instructions (Biacore AB, Uppsala, Sweden). His_6-Cdk2/CycA (5−50 nM) was bound to an NTA chip in running buffer (10 mM HEPES (pH 7.5), 150 mM NaCl, 50 μM EDTA, 0.005% surfactant P-20, and 4 mM β-mercaptoethanol) to yield ~700 reflectance units and a stable baseline. Phosphatase was injected at varying concentrations (0.1−4 μM) in the running buffer, and the observed rates and signal intensities were independent of the flow rate (20−50 μL/min). Injection of concentrations of Cdc25B >4 μM yielded nonspecific binding to the chip, precluding a more thorough analysis of the slowly associating mutant R492L. Observed reflectance units were corrected by subtraction of a small nonspecific signal (<5%) using a reference cell consisting of an NTA chip without bound Cdk2/CycA.

Data Fitting. Equations cited in the results were fitted to the data using weighted least-square fitting in Excel (Microsoft).

RESULTS

Association and Chemistry of Cdc25B. We have probed the detailed reaction mechanism of Cdc25 phosphatase with its native Cdk2-pTpY/CycA substrate. The Cdc25 phosphatases preferentially dephosphorylate pThr14 and complete this reaction prior to engaging the second phosphate, pTyr15 (*14*). We limit our present study to the phosphorolysis of this first phosphate monoester because it is the initial substrate that the enzyme encounters. For data analysis and interpretation, we use Scheme 1, which involves three steps. The formation of the enzyme−substrate (E·S) complex is governed by the rates of association (k_{on}) and dissociation (k_{off}). Phosphate transfer from pThr14 of Cdk2-pTpY/CycA to Cys473 of Cdc25B to form the phospho-enzyme intermediate (E~P) with concomitant release of protein product (Cdk2-TpY/CycA) is governed by k_2 and is considered irreversible on the basis of precedent in the field (*11*). Hydrolysis of the acid-labile phospho-enzyme intermediate is governed by k_3. We do not observe a burst of phosphate formation at high concentrations of enzyme and Cdk2-pTpY/CycA substrate (data not shown), indicating that neither hydrolysis of the phospho-enzyme nor release of protein product is rate-limiting. Therefore, single-turnover kinetics are an ideal tool for elucidating the microscopic rate constants for the first half reaction of the catalytic cycle performed by Cdc25B, namely, the formation of the E·S complex followed by the chemical step of phosphate transfer leading to the phospho-enzyme intermediate. For all single-turnover reactions under limiting conditions, a single first-order exponential is used to fit the data for the appearance of phosphate arising from either final product formation or the acid-labile phospho-enzyme intermediate,

$$[P_i] = [S](1 - e^{-k_{obs}t}) \quad (1)$$

wherein $[P_i]$ is the concentration of inorganic phosphate, $[S]$ is the total amount of substrate, and k_{obs} is the observed rate constant. Under limiting low concentrations of both enzyme and substrate yet keeping $[E] \gg [S]$, the association of enzyme and substrate is rate limiting ($k_{on}[E] \ll k_2$) and k_{obs} is proportional to enzyme concentration yet independent of the substrate concentration. At limiting high enzyme concentrations, the E·S complex accumulates rapidly ($k_{on}[E] \gg k_2$), and k_{obs} becomes independent of enzyme concentration, reflecting the rate-limiting chemical step ($k_{obs} = k_2$).

To measure the rate of association of Cdc25B with its protein substrate Cdk2-pTpY/CycA, we performed single-turnover experiments at low concentrations of both enzyme and substrate while minimally maintaining a 5-fold excess of Cdc25B over Cdk2-pTpY/CycA. The rate of appearance of inorganic phosphate for each reaction was well described by a single-exponential equation (eq 1, Figure 1A). The k_{obs} values were directly proportional to enzyme concentrations yet independent of substrate concentrations (Figure 1, insert). The rate constant for association (k_{on}) can be obtained from the linear plot of k_{obs} versus enzyme concentrations as defined by

$$k_{obs} = k_{on}[E] + k_{off} \quad (2)$$

The second-order rate constant for association, $k_{on} = (1.3 \pm 0.3) \times 10^6\ M^{-1}\ s^{-1}$, is essentially equal to the specificity constant $k_{cat}/K_m = 9 \times 10^5\ M^{-1}\ s^{-1}$ (*14*, *15*), indicating that under dilute conditions, substrate association is the rate-determining step (Table 1). This observed rate constant for substrate association is the first to be reported in the family of protein phosphatases and is within the range of association rate constants measured for other protein−protein complexes (10^5−$10^9\ M^{-1}\ s^{-1}$) (*25*−*27*). The rate constant for the dissociation of the substrate (k_{off}) could not be determined from this experiment because it is slow compared to the time course of the reaction (Figure 1A, insert). In fact, the apparently slow dissociation of substrate suggested that the kinetic mechanism for Cdc25B may better be described by two consecutive irreversible steps.

To probe this possibility, we used rapid quench to perform single-turnover experiments at higher enzyme and substrate concentrations, still minimally maintaining a 5-fold excess of Cdc25B over Cdk2-pTpY/CycA. For enzymes with sticky substrates like Cdc25B, there exists a characteristic lag in phosphate formation at moderate enzyme concentrations ($k_{on}[E] \geq k_2$) under single-turnover conditions (*28*, *29*). If catalysis proceeds through an irreversible pseudo-first-order reaction (pseudo-irreversible binding, where k_{off} is finite but

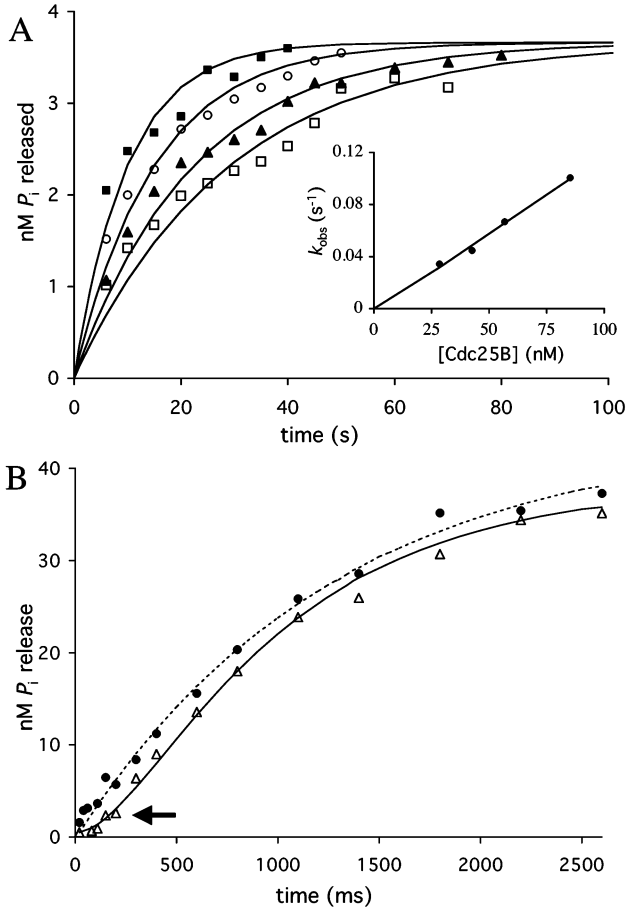

FIGURE 1: Single-turnover kinetics of the Cdc25B-catalyzed dephosphorylation of Cdk2-pTpY/CycA. (A) Cdk2-pTpY/CycA (4 nM) was mixed with varying concentrations of Cdc25B (28 nM, □; 42 nM, ▲; 56 nM, ○; 85 nM, ■) under manual quench conditions. The single first-order exponential (eq 1) was fitted to each data set, and the k_{obs} were re-plotted vs enzyme concentration, as shown in the inset, to derive $k_{on} = (1.3 \pm 0.3) \times 10^6$ M^{-1} s^{-1}. (B) Cdk2-pTpY/CycA (50 nM) was mixed with moderate (2 μM, △) and high (20 μM, ●) concentrations of Cdc25B under rapid quench conditions. The data for 2 μM enzyme were fitted with two first-order exponential equations (eq 3) with $k_{on} = 1.3 \times 10^6$ M^{-1} s^{-1} and $k_2 = 0.9$ s^{-1}. The data for 20 μM enzyme were fitted with one first-order exponential (eq 1) with $k_2 = 1.2$ s^{-1}. All data shown are representative of four independent experiments performed with different concentrations of the substrate and enzyme.

Table 1: Summary of Kinetic Parameters

parameters/ enzyme	k_{on} ($\times 10^3$ M^{-1} s^{-1})	k_{cat}/K_m[a] ($\times 10^3$ M^{-1} s^{-1})	k_2 (s^{-1})
wild type	1300 ± 300	860 ± 180	1.1 ± 0.1
C473S	330 ± 80		
R488L	7.1 ± 0.4	1.3 ± 0.3	≥0.3
R488A	3.1 ± 0.3	1.0 ± 0.4	≥0.3
R492A	60 ± 7	25 ± 2	~1.2
R492L	6.4 ± 0.5	4.2 ± 0.5	0.016 ± 0.004
R492K	0.3 ± 0.1	0.32 ± 0.05	~0.04
Y497A	6.5 ± 0.6	4.5 ± 0.7	0.14 ± 0.03
Y497T	7.0 ± 0.9	2.5 ± 0.6	n.d.
Y497F	n.d.	100 ± 20	0.9 ± 0.2
D206A	1.4 ± 0.4	2 ± 0.2	0.12 ± 0.02

[a] The data for k_{cat}/K_m shown for comparison purposes were originally published in refs 15, 16, and 35.

very slow) followed by an irreversible first-order reaction (chemistry), product formation can be described by the following equation.

$$[P_i] = [S]\left[1 + \frac{1}{k_{on} - k_2}(k_2 e^{-k_{on}t} - k_{on} e^{-k_2 t})\right] \quad (3)$$

At the beginning of the reaction, phosphate formation is limited by the association between enzyme and substrate (lag), whereas for later time points, the observed rate of phosphate formation is governed by the rate of chemistry. In agreement with this prediction, we observed a clear lag of phosphate formation at the early phase of the reaction at moderate concentrations of Cdc25B (1−2 μM) (Figure 1B). In contrast, at high concentrations of enzyme (~20 μM), the appearance of phosphate can be described by a single-exponential equation (eq 1, Figure 1B), and the k_{obs} values are independent of both enzyme and substrate concentrations, indicative of rate-limiting chemistry ($k_{obs} = k_2 = 1.1 \pm 0.1$ s^{-1}, Scheme 1). For the reaction at 2 μM Cdc25B, eq 3 can be well fitted to the data using $k_{on} = (1.3 \pm 0.2) \times 10^6$ M^{-1} s^{-1} as the pseudo-irreversible rate constant for association and $k_2 = 0.9 \pm 0.1$ s^{-1} as the rate constant for phosphate transfer, consistent with the values of k_{on} and k_2 obtained under the limiting lower and higher enzyme concentrations, respectively.

To further validate the kinetic parameters from these single-turnover experiments, we compared them to previously determined steady-state parameters. First, in a kinetic scheme where k_{off} is small compared to k_2, k_{on} is equal to k_{cat}/K_m, as noted above (Table 1). Thus,

$$k_{cat} = \frac{k_2 k_3}{k_2 + k_3} \approx \frac{k_2}{2}, \text{ when } k_2 \approx k_3 \quad (4)$$

which is in good agreement with our previously determined k_{cat} of 1.2 s^{-1} (*30*), the k_2 of 1.1 s^{-1} determined here, and the k_3 of 0.8 s^{-1} reported previously (*30*). Finally, the apparent Michaelis constant determined by steady-state kinetics (440 ± 80 nM) (*15*), is in good agreement with the one obtained mathematically (K_m = 423 nM) using the following equation.

$$K_m = \frac{k_2 k_3}{k_{on}(k_2 + k_3)} \approx \frac{k_2}{2k_{on}}, \text{ when } k_2 \approx k_3 \quad (5)$$

Substrate-Trapping Mutant C473S. As shown above, we were not able to obtain a reliable value for the rate constant for dissociation of the E·S complex (k_{off}), although it is clearly less than the rate constant for phosphate transfer (k_2). This slow dissociation implies that the Michaelis constant (K_m) is not reflective of the true binding affinity of Cdc25B toward the protein substrate. Therefore, to probe the binding kinetics of Cdc25B to its protein substrate, we attempted to estimate a true value for K_d or k_{off} using the substrate-trapping mutant of Cdc25B. Like other members of the protein tyrosine phosphatase family, a substrate-trapping mutant of Cdc25B can be generated by substituting the active site cysteine with a serine (C473S). It has been previously demonstrated that the C473S mutant has a strong binding affinity toward physiological protein substrates (*15*, *31*). Moreover, we have shown that the crystal structure of C473S is essentially identical to wild-type Cdc25B with an overall rmsd for all backbone atoms of 0.23 Å and for the active site loop of 0.13 Å (*16*).

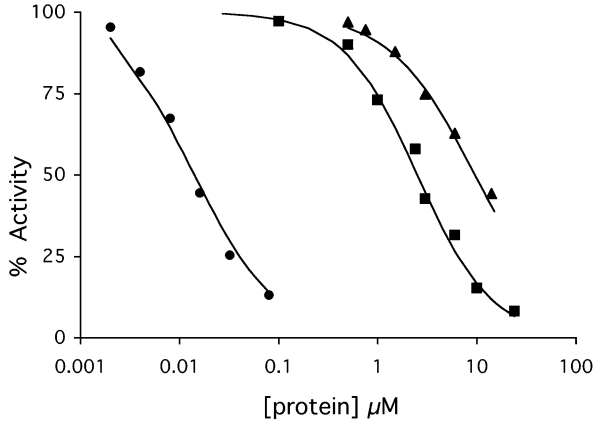

FIGURE 2: Competition binding assays. The affinity of C473S for Cdk2-pTpY/CycA was determined by measuring its inhibition of the reaction with wild-type Cdc25B. The IC_{50} of C473S (varying 2−80 nM) was determined using Cdk2-pTpY/CycA (3 nM) and Cdc25B (0.5 nM) with fitting by eq 6. The affinity of Cdk2/CycA for Cdc25B was determined by measuring its inhibition of the reaction with Cdk2-pTpY/CycA. The IC_{50} of Cdk2/CycA (varying 0−15 μM) was determined by using Cdk2-pTpY/CycA (70 nM) and Cdc25B (5 nM) with fitting by eq 8. The fitted IC_{50} values for C473S (●) and the unphosphorylated product (Cdk2/CycA, ▲) are 13 ± 2 nM and 12 ± 3 μM, respectively. The data for inhibition by C473D from (*15*) is shown for comparison (■). The data shown are the mean values of at least three separate experiments.

First, to accurately determine the true binding affinity of C473S (K_d), we performed a competitive binding assay, wherein varying concentrations of C473S are used to sequester the Cdk2-pTpY/CycA substrate from wild-type Cdc25B (Figure 2). In previous experiments, we found that we were simply titrating the substrate. The observed IC_{50} values were equivalent to half the concentration of substrate in the experiment, consistent with stoichiometric binding between Cdk2-pTpY/CycA and C473S (*15*); data not shown). We have raised the specific radioactivity of the substrate 10-fold so as to measure the true affinity by performing these measurements at lower concentrations of Cdk2-pTpY/CycA (3−6 nM). Because the concentrations of C473S were not 10-fold greater than the substrate concentration, the modified Morrison equation (*32*)

$$100^{*}\frac{v_i}{v_0} = 1 - \frac{([S] + [I] + IC_{50}) - \sqrt{([S] + [I] + IC_{50})^2 - 4[S][I]}}{2[S]} \quad (6)$$

wherein [*S*] is the concentration of Cdk2-pTpY/CycA, was used to fit the percent activity (100* v_i/v_0) observed at each concentration of C473S ([*I*]). The observed IC_{50} is 13 ± 2 nM and is independent of the concentration of the wild-type enzyme used in the trap. To convert the IC_{50} value to K_i, we cannot apply the Cheng−Prusoff equation (*33*) because C473S sequesters the substrate, not the enzyme. Instead, the binding constant (K_i) of a competitive inhibitor for the substrate can be extracted from the IC_{50} value through $K_i = IC_{50} - [S]/2$ (*34*). The observed IC_{50} is essentially equal to the true K_i ($= K_d \approx 10$ nM) under our experimental conditions because the substrate concentration (≤6 nM) is less than the observed IC_{50}.

To investigate whether C473S serves as a good kinetic mimic of wild-type Cdc25B in forming the E·S complex,

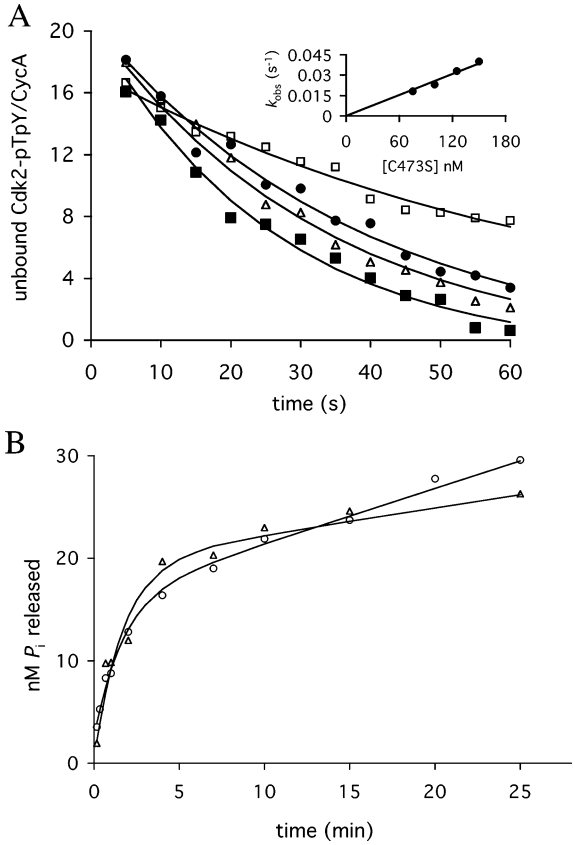

FIGURE 3: Association and dissociation of C473S. (A) C473S (75−150 nM) was mixed with Cdk2-pTpY/CycA (20 nM) and initially quenched with wild-type Cdc25B (3 μM) followed by a subsequent quench with 30% TCA. The concentrations of C473S shown are 75 nM (□), 100 nM (●), 125 nM (△), and 150 nM (■). The data shown are representative of two independent experiments performed in duplicate, and moderate changes in the concentrations of the wild type used in the initial quench (2−4 μM) do not affect the results (data not shown). The k_{obs} values shown in the inset are the mean values for each concentration of C473S (error ≤15%) and yield a k_{on} of 3×10^5 M^{-1} s^{-1}. (B) C473S (210 nM) complexed with Cdk2-pTpY/CycA (63 nM) was incubated with wild-type Cdc25B (10 μM, △, 20 μM, ○) for varying lengths of time. The data shown are representative of four independent measurements under similar reaction conditions. The k_{off} determined using eq 7 is 0.010 ± 0.003 s^{-1}.

we next measured the rate of association of C473S with Cdk2-pTpY/CycA (Figure 3A). In this experiment, C473S and the protein substrate were mixed at concentrations above the K_d derived from the competitive binding assay above. Subsequent addition of a large molar excess of wild-type Cdc25B was used to trap and dephosphorylate any unbound Cdk2-pTpY/CycA as a function of time. This trapping reaction was then quenched by the addition of acid. The concentration of the wild-type enzyme and its incubation time in the first quench were carefully chosen to ensure complete dephosphorylation of pThr14 from the unbound substrate while minimizing the dissociation of substrate from C473S (also, see below). The first-order exponential of eq 1 was modified and fitted to the time-dependent depletion of free Cdk2-pTpY/CycA. The second-order rate constant for association was obtained from the linear plot of k_{obs} values versus C473S concentrations (Figure 3A, inset). As expected from the essentially identical crystal structures of wild-type Cdc25B (*13*, *22*) and its C473S mutant (*16*), the rate constant for the association of C473S (3.3×10^5 M^{-1} s^{-1}) is relatively

Table 2: Data Collection and Refinement Statistics for the Structure Determination of the C473D and R492L Mutants of Cdc25B

parameter	C473D	R492L
space group	$P2_12_12_1$	$P2_12_12_1$
unit cell	$\alpha = 40.89$ Å $\beta = 71.19$ Å $\chi = 73.87$ Å $\alpha = \beta = \gamma = 90°$	$\alpha = 49.96$ Å $\beta = 71.32$ Å $\chi = 75.06$ Å $\alpha = \beta = \gamma = 90°$
temperature of data collection	100 K	100 K
resolution	1.6 Å	2.0 Å
no. of reflections	34,010	18,160
redundancy[a]	7.1 (5.9)	7.0 (5.2)
R_{sym}[a,b]	8 (35)	10 (29)
completeness	96.0%	97.0%
average I/σ[a]	32.8 (4.3)	25 (5)
R_{work}[c]/R_{free}[d]	18.0%/19.6%	18.7%/21.0%
RMS bond length deviation from ideal geometry	0.005	0.005
RMS bond angle deviation from ideal geometry	1.3	1.3
Ramachandran statistics	97% in favored regions 100% in allowed regions	97% in favored regions 100% in allowed regions
no. of protein atoms	1429	1452
no. of water molecules	216	145
no. of sulfate molecules	1	1
no. of chloride ions	2	2
no. of protein residues with alternate conformations	5	5

[a] The numbers in parenthesis describe the relevant value for the highest resolution shell. [b] $R_{sym} = \Sigma|I_i - \langle I\rangle|/\Sigma I$, where I_i is the intensity of the ith term observed, and $\langle I\rangle$ is the mean intensity of the reflections. [c] $R_{work} = \Sigma||F_{obs}| - |F_{calc}||/\Sigma|F_{obs}|$, which was calculated using 90% of the reflections against which the model was refined. [d] $R_{free} = \Sigma||F_{obs}| - |F_{calc}||/\Sigma|F_{obs}|$, which was calculated using the test set consisting of 10% of the total reflections, randomly selected from the original data set.

similar to the wild type value (1.3×10^6 M^{-1} s^{-1}) (Table 1).

Having validated the use of C473S as a kinetic mimic of wild-type Cdc25B, we measured the rate of its dissociation from the substrate so as to estimate the rate constant for dissociation of the E·S complex. After preforming the C473S·Cdk2-pTpY/CycA complex, the dissociation of C473S can be detected by measuring the time-dependent accumulation of the free substrate, as trapped by wild-type Cdc25B. Because of the high affinity and rapid reassociation of C473S, a very high concentration of the wild-type enzyme (≥ 10 μM) was needed. We expected to use eq 1 describing the simple exponential accumulation of phosphate to fit our data. Instead, we observed biphasic kinetics and needed to use

$$[P_i] = [S](1 - e^{-k_{obs}t}) + \beta t \quad (7)$$

to fit the data (Figure 3B). As expected, the observed rate of the exponential component of phosphate formation was independent of the absolute concentration of the preformed complex and independent of the concentration of wild-type Cdc25B in the quench (data not shown). In contrast, the linear rates (β) were directly proportional to the amount of wild-type Cdc25B used in the trap. The amplitude of the fast exponential phase varied from 13 to 30% of total substrate used, and the derived rate constant for dissociation of C473S is 0.010 ± 0.003 s^{-1}, yielding a half-life for dissociation of the complex of ~70 s. Extended incubations (>2 h) of the pre-bound substrate yielded complete dephosphorylation in the second slower phase, which we cannot explain (data not shown). Because this second slower rate is dependent on the concentration of wild-type Cdc25B, our data for the fast step, albeit not accounting for all of the substrate, should still reflect the correct rate constant for the release of Cdk2-pTpY/CycA from the C473S mutant.

The kinetic data describing the association, dissociation, and binding affinity of the C473S mutant to Cdk2-pTpY/CycA that we obtained in these three experiments are in agreement with one another. The calculated K_d of C473S (~30 nM) obtained by the ratio between k_{off} (Figure 3B) and k_{on} (Figure 3A) is remarkably close to the K_d (~10 nM) determined in the competitive binding experiment (Figure 2). Comparing C473S to the wild type, the similar k_{on} values (3×10^5 M^{-1} s^{-1} vs 1.3×10^6 M^{-1} s^{-1}) suggest that C473S is a reasonable mimic of the wild type not only structurally but also kinetically during the formation of an E·S complex. Thus, if we assume a similar k_{off} (~ 0.01 s^{-1}) for the E·S complex, consistent with the apparent irreversibility of substrate association (Figure 1), then we arrive at an estimated K_d for the E·S complex of ~10 nM.

Interactions at the Remote Docking Site Affect k_{on} and/or k_2. To better understand the roles of the hotspot residues in the remote docking site during the catalysis of the protein substrate by Cdc25B phosphatase, we next investigated the kinetics of various hotspot mutants. In particular, we were interested in the most important residue in this cluster, namely, Arg492 of Cdc25B (*16*, *35*).

Mutations of Arg492. Although we have demonstrated that activities with small molecule substrates that interact only at the active site are mostly unaffected by the hotspot mutations on Cdc25B (*15*), it is possible that more global changes in structure have occurred that could complicate any mechanistic interpretations. Thus, we began by determining the crystal structure of R492L. The structure of R492L was solved to 2.0 Å resolution, with an R/R_{free} of 18.6/20.1 (Table 2). The R492L mutant crystallized in the same space group ($P2_12_12_1$) and under the same conditions as those for wild-

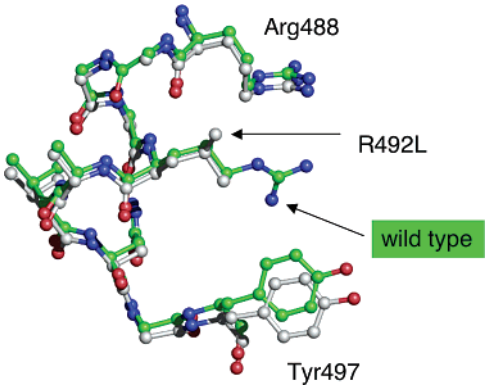

FIGURE 4: Hotspot region from the crystal structure of R492L (in gray) overlaid with wild-type Cdc25B (in green).

type Cdc25B and the crystal structure confirms that no significant changes in structure occurred as a result of this mutation. The overall rmsd of wild-type Cdc25B versus R492L for all backbone atoms is 0.26 Å. As expected from the wild-type level of activity with small molecule substrates for R492L, the active site loops are also superimposable, with an rmsd for the Cα and all atoms of residues 473−479 of 0.12 and 0.23 Å, respectively. In the crystal structure, a sulfate ion that mimics the phosphate from a bound substrate is seen in the active site, as also observed for the wild-type protein and the C473S mutant. In the wild-type protein, Arg492 is found coordinated to a sulfate ion by two hydrogen bonds, possibly mimicking the interaction with Asp206 of the protein substrate Cdk2-pTpY/CycA. The R492L mutant does not contain this sulfate. The conformation adopted by Leu492 is close to the most preferred rotamer with the angles χ_1 and χ_2 of Leu492 rotated by 10° and 30°, respectively, because of close packing with the nearby Arg488 (Figure 4). The Cβ, Cγ, and Cδ2 atoms of the substituted Leu492 are in the same positions as the Cβ, Cγ, and Cδ2 atoms of wild-type Arg492. The interaction between Arg488 and Leu492 prevents Arg488 from adopting a conformation wherein its guanidino group could substitute for the loss of the guanidino group of Arg492. The effects of this mutation are, therefore, not global but solely encompass the loss of the guanidino group of Arg492.

We next measured the association of R492L with the protein substrate using single-turnover kinetics under low concentrations of both enzyme and substrate yet keeping [*E*] ≫ [*S*], where the association of enzyme and substrate is rate limiting (k_{on} [*E*] ≪ k_2). Our initial expectation was that the hotspot mutants would possess an essentially equivalent rate of association for the E•S complex yet dissociate more rapidly. We were, therefore, surprised to find that R492L displayed a 200-fold slower rate constant for association (6400 ± 500 M^{-1} s^{-1}) compared to that of wild-type Cdc25B, comparable to its steady-state k_{cat}/K_m (4200 M^{-1} s^{-1}) (Figure 5A, Table 1). As for the wild type, the rate of dissociation appeared too close to zero to be determined in this experiment. At high concentrations of R492L (>3 μM), the observed rate of product formation could also be described by a single exponential (eq 1) and was independent of enzyme concentration to yield a k_2 of 0.016 ± 0.004 s^{-1}, nearly 100-fold slower than that for wild-type Cdc25B (Figure 5B, Table 1). To ensure that the slowed rate of phosphate transfer did not reflect a change in substrate selection (pThr14 vs pTyr15), we performed phospho-amino

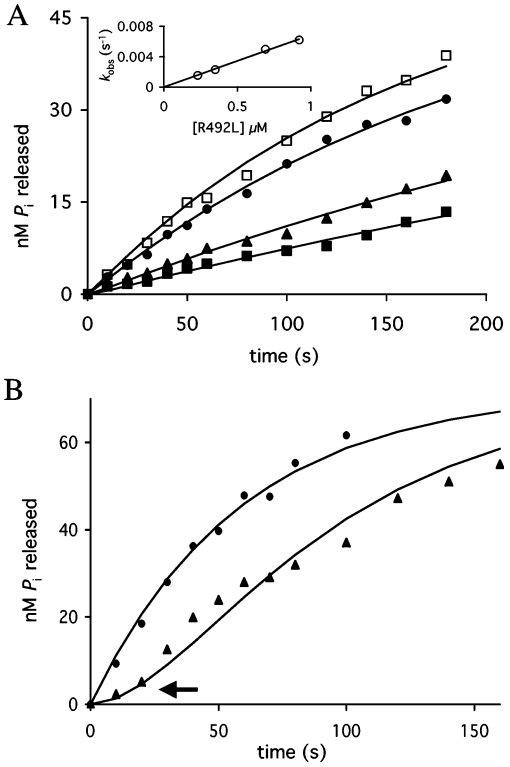

FIGURE 5: Single-turnover kinetics of R492L. (A) Cdk2-pTpY/CycA (40 nM) was mixed with varying concentrations of R492L (0.2 μM, ■; 0.3 μM, ▲; 0.7 μM, ●; 0.9 μM, □) under manual quench conditions, and product formation was monitored. Equation 1 was fitted to each progress curve to yield observed rates that were further analyzed as shown in the inset to yield a rate constant for association of 6400 ± 500 M^{-1} s^{-1}. (B) Cdk2-pTpY/CycA (70 nM) was mixed with moderate (1.5 μM, ▲) and high (15 μM, ●) concentrations of R492L under manual quench conditions. The data for 1.5 μM enzyme were fitted with two first-order exponential equations (eq 3) with $k_{on} = 1.6 \times 10^4$ M^{-1} s^{-1} and $k_2 = 0.16$ s^{-1}. The data for 15 μM enzyme were fitted with one first-order exponential (eq 1) with $k_2 = 0.12$ s^{-1}. Data shown are representative of at least four independent experiments.

acid analysis on the dephosphorylated product to demonstrate the loss of pThr and the retention of pTyr (data not shown), as seen previously for the wild type (*14*). The calculated K_m of 1.3 μM (eq 5) obtained from these significantly perturbed values for k_2 and k_{on} is in reasonable agreement with the experimentally determined K_m under steady-state conditions (~3 μM, data not shown). From these data, we expected R492L, like wild-type Cdc25B (Figure 5B), to exhibit a distinct lag in product formation at intermediate concentrations of the substrate. Indeed, we observed such a lag, and the rate constants derived from fitting eq 3 to these data (k_{on} = 1.6×10^4 M^{-1} s^{-1}, k_2 = 0.016 s^{-1}) are consistent with our previous measurements under limiting conditions (Figure 5B).

Similar single-turnover experiments under limiting low concentrations of enzyme with the more and less deleterious R492K and R492A mutants, respectively, again showed reasonable correlations between k_{on} and k_{cat}/K_m (Table 1). At higher concentrations of enzyme, lag phases could be detected yielding estimated k_2 values of 0.04 and 1.2 s^{-1} for R492K and R492A, respectively. Thus, different substitutions for Arg492 yield different rate constants for association and subsequent chemistry. In particular, despite being the most dramatic perturbation in terms of residue type, the R492A

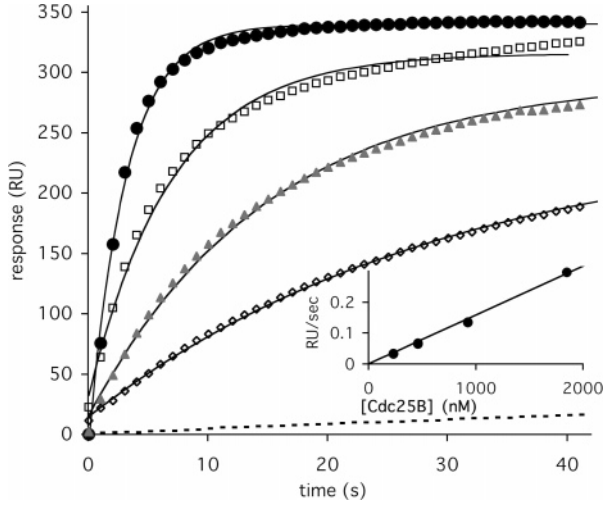

FIGURE 6: Biacore binding experiment. The binding of Cdc25B to the protein product was monitored by Biacore. For wild-type Cdc25B, binding at concentrations of 230 nM (◊), 460 nM (▲), 925 nM (□), and 1900 nM (●) are shown along with curves fitted to eq 1. The inset shows the concentration dependence of k_{obs} on Cdc25 and was used to derive a rate constant for association of $(5.6 \pm 0.7) \times 10^5$ M^{-1} s^{-1}. For R492L, binding at 1900 nM is shown as a dashed line near the bottom of the graph.

mutant did not show a change in k_2 compared to that of wild-type Cdc25B (Table 1).

We were interested in obtaining independent confirmation for the dramatic reduction in rate constants for association seen for our hotspot mutants in comparison to that of wild-type Cdc25B. It is possible that we observe slower association for the hotspot mutants only because we use catalysis as a read-out of binding and thereby cannot detect nonproductive complex formation. Although a direct comparison with E·S formation is not possible using Biacore because of the subsequent catalytic event, we use this technique to probe the association between the enzyme and the dephosphorylated protein product Cdk2/CycA. (Note that this binding event does not reflect the dissociation of E·P because true product departure occurs from the phospho-enzyme intermediate, not the unmodified enzyme.) Limitations of this approach include the potential differences between surface chemistry (Biacore) versus solution chemistry (enzyme assays) and a smaller range of useable enzyme concentrations (Materials and Methods). We observed association between wild-type Cdc25B and its protein product Cdk2/CycA that could be fitted with a single exponential (Figure 6, eq 1). By varying the concentration of Cdc25B, we derived a second-order rate constant for this rate of association of $(5.6 \pm 0.7) \times 10^5$ M^{-1} s^{-1}, in reasonable agreement with the observed rate of association between the enzyme and substrate (Figure 6, inset). Under identical conditions, the R492L mutant associates at least 200-fold more slowly (Figure 6), consistent with our single-turnover experiments (Table 1).

Single-Turnover Kinetics: Mutations of Arg488. Like R492L, R488L associates with the protein substrate with a significantly reduced second-order rate constant (7100 M^{-1} s^{-1}) compared to that of wild-type Cdc25B (Figure 7A, Table 1). As for wild-type Cdc25B and R492L, the dissociation of the E·S complex did not occur rapidly because the intercept in the replot was not distinguishable from zero (Figure 7A, insert). Attempts to determine the rate of chemistry for R488L by saturating the E·S complex at higher

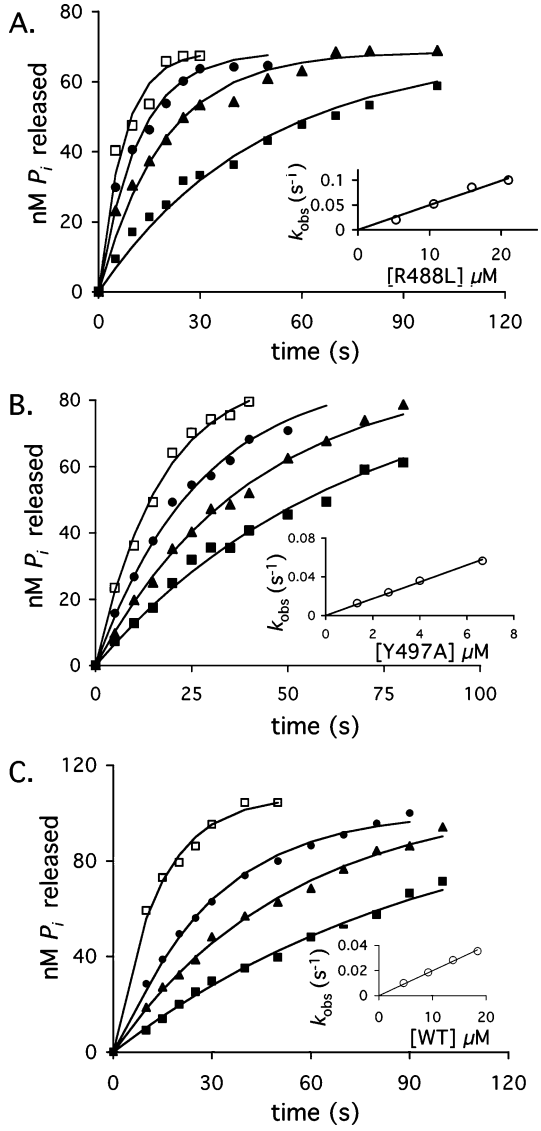

FIGURE 7: Single-turnover kinetics of other hotspot mutants. Cdk2-pTpY/CycA (60−100 nM) was mixed with varying concentrations of (A) R488L (5 μM (■), 11 μM (▲), 16 μM (●), and 21 μM (□)) or (B) Y497A (1.3 μM (■), 2.7 μM (▲), 4 μM (●), and 6.7 μM (□). (C) The D206A mutant of the protein substrate was mixed with wild-type Cdc25B at 4.6 μM (■), 9.2 μM (▲), 13 μM (●), and 18 μM (□). Equation 1 was fitted to each progress curve to yield observed rates that were further analyzed as shown in the insets to derive the rate constants for association listed in Table 1. Data shown are representative of at least four independent experiments.

concentrations of enzyme were not feasible. We observed a linear dependence of k_{obs} on increasing enzyme concentrations up to 25 μM (Figure 7A, insert), suggesting that the rate of chemistry is not as perturbed for the R488L mutant as that observed for the R492L mutant (Table 1). As expected from steady-state measurements (*35*), R488A behaved in a manner similar to that of R488L in the single-turnover experiments (Table 1).

Single-Turnover Kinetics: Mutations of Tyr497. Like R488L and R492L, Y497A showed a significantly slower rate constant for association (6500 M^{-1} s^{-1}) compared to that of the wild type, as also reflected in the steady-state k_{cat}/K_m value (Figure 7B, Table 1). Also, as for R488L, no dramatic increase in k_{off} compared to that of the wild type was detected from the linear plots of k_{obs} versus enzyme

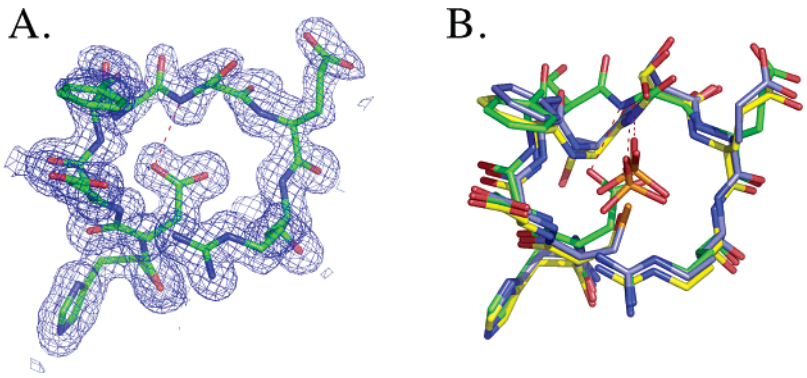

FIGURE 8: Crystal structure of C473D. (A) The active site of the C473D mutant is shown with electron density contoured at one sigma. The hydrogen bond between Asp473Oδ1 and the amide of Ser477 is indicated by a dotted line. (B) Overlay of C473D (carbon atoms in green), wild-type Cdc25B (carbon atoms in purple), and C473S (carbon atoms in yellow). The hydrogen bonds from the amide backbone of Ser477 to the sulfate or Asp473 are indicated by dotted lines.

concentrations. Unlike R488L, sufficiently high concentrations of Y497A (>100 μM) under single-turnover conditions showed saturation in k_{obs}, and the derived rate constant for chemistry ($k_2 = 0.14$ s^{-1}) is almost 10-fold slower than that for wild-type Cdc25B (Table 1). As expected from steady-state measurements (*35*), Y497T showed the same rate constant for association as Y497A (Table 1). Interestingly, Y497F, which is more similar to the wild type in k_{cat}/K_m, was also more similar in k_2, as determined under saturating concentrations of the enzyme (Table 1).

Single-Turnover Kinetics: Mutation of Asp206. We have previously shown that Asp206 of Cdk2 is the corresponding hotspot residue of the protein substrate that interacts with Arg488 and more significantly with Arg492 (*16*, *35*). The measured k_{cat}/K_m of wild-type Cdc25B using the D206A mutant was ~600-fold slower compared to that of the wild-type substrate, and double mutant cycle analysis revealed interaction energies between Asp206 of Cdk2 and Arg488 and Arg492 of Cdc25B of 2.8 and 3.9 kcal/mol, respectively. Moreover, we were able to restore significant activity by swapping the hotspot residues between the enzyme and substrate (i.e., R492D of Cdc25B with D206R of Cdk2). To further investigate the role of Asp206, we performed single-turnover experiments with the D206A mutant of the substrate using wild-type Cdc25B. Given the well-established interaction between Asp206 and the two arginines of the enzyme, we were not surprised to find the rate constant for association of D206A with wild-type Cdc25B to be significantly slowed (~1000-fold) compared to the wild-type protein substrate, again in good agreement with the steady state k_{cat}/K_m (Figure 7C, Table 1). Under sufficiently high concentrations of enzyme (>50 μM), the observed rate under single-turnover conditions revealed a k_2 for D206A that was about 10-fold slower than that for the wild-type substrate (Figure 7C, Table 1). The measured kinetic parameters for D206A resemble those seen for the hotspot mutants of Cdc25B, consistent with the proposal that Asp206 of the protein substrate is involved in the same step(s) of the reaction as the hotspot residues of the enzyme.

Interactions at the Active Site Affect k_{off}. The absence of an observed burst of formation of inorganic phosphate with protein substrate suggests rapid hydrolysis of the phospho-enzyme intermediate. Given the tight packing and exclusion of water in the active site region that we observe in the docked model of C473S bound to Cdk2-pTpY/CycA (*16*), we would expect dissociation of the protein product prior to phospho-enzyme hydrolysis, as shown in Scheme 1. To further probe these kinetic events, we turned first to the C473D mutant. In contrast to the so-called substrate-trapping mutant C473S, the C473D mutant has ~150-fold lower affinity toward the protein substrate (13 nM vs 2 μM) (Figure 3).

We began by determining the crystal structure of the C473D mutant to 1.6 Å resolution, with an R/R_{free} of 18.0/19.6 (Table 2). No significant changes in overall structure occurred as a result of this mutation with an overall rmsd of wild-type Cdc25B versus C473D for all backbone atoms of 0.29 Å. Significant differences are seen only in the active site loop with an rmsd for all atoms of residues 473−479 of 1.03 Å. The active site loop, instead of adopting the unusual geometry that is ideally suited for binding phosphate from the substrate, is partially closed over the active site (Figure 8). In fact, in contrast to the wild type and C473S, both of which have a tightly bound sulfate in the active site (*22*), the C473D mutant does not have an active site ligand. This change in conformation of the active site loop is due to both steric repulsion and the formation of alternative hydrogen bonds between backbone amides and oxygen atoms of the Asp473 side chain. Specifically, the Oδ1 atom of Asp473 would interfere with the main chain amide group of Ser476, if it were in the wild-type conformation. The resulting rearrangement of residues 475−478 allows for a new hydrogen bond between the amide group of Ser477 and the Oδ1 atom of Asp473 (2.9 Å). Also, Ser477, which in the wild-type structure uses its inward facing amide to form a hydrogen bond with an oxygen atom of the bound sulfate, in C473D adopts a conformation that would sterically interfere with a bound sulfate. The distortion of the active site loop in C473D extends to a comparison with the apo structure (*22*). In the apo structure, the active site loop is seen preformed to bind phosphate, with three water molecules that make hydrogen bonds similar to three of the oxygen molecules of the sulfate. Although two of these water molecules are still present in the C473D mutant, the one that hydrogen bonds to Ser477 is missing. Thus, it is clear that the weaker affinity of the C473D mutant arises from the distortion in the active site loop, where binding of phosphate is not possible.

Kinetically, this 150-fold weaker binding of C473D compared to C473S can arise from a faster k_{off}, a slower k_{on},

or both simultaneously. To test which of these might be the dominating difference, we first attempted to measure the rate of dissociation of C473D from the Cdk2-pTpY/CycA substrate using the protocol we had developed for the C473S mutant. After presumably forming a complex with Cdk2-pTpY/CycA in the presence of 30 μM C473D (15 $\times$ K_i), excess wild-type Cdc25B was added to capture any substrate released from the complex. We found complete conversion to product in the shortest time point possible ($\sim$4 s) (data not shown). Thus, in stark contrast to the slow dissociation of C473S with a half-life of $\sim$70 s (Figure 5), the rate constant for the dissociation for C473D under the same reaction conditions was too fast to be measured, with a half-life $<$2 s. Thus, the k_{off} for C473D is at least 35-fold greater than that for C473S, accounting for the majority of the difference in binding affinity. We conclude that the weaker binding for C473D is due to a loss of productive interactions in the active site region and is mediated by a faster k_{off}, consistent with the fast dissociation of the protein product from the phospho-cysteine intermediate.

To further test the role of interactions at the active site, we next investigated the affinity of the completely dephosphorylated protein product. A comparison of the crystal structure of Cdk2-pTpY/CycA (Russo, Rudolph, and Pavletich, unpublished data) with Cdk2/CycA reveals no significant changes, although the exact orientations of the phosphates of pThr14 and pTyr15 could not be resolved. Using Cdk2/CycA as an inhibitor of the Cdc25B reaction, we determined an IC_{50} of 12 $\pm$ 3 μM (Figure 3) using the folowing equation.

$$\% \text{ Activity} = \frac{100}{\left(1 + \frac{[Cdk2/CycA]}{IC_{50}}\right)} \quad (8)$$

Thus, the affinity for Cdk2/CycA is 3 orders of magnitude weaker than the K_d we have estimated for Cdk2-pTpY/CycA using the C473S mutant ($\sim$15 nM). These results again suggest that the absence of favorable interactions between the active site of Cdc25B and its protein product is largely responsible for this decrease in binding affinity. We were unable to measure the rate constant for dissociation of the unphosphorylated product from Cdc25B because it was not possible to obtain sufficiently high concentrations of the protein product to ensure the preformation of a complex.

DISCUSSION

Hotspots and the Rate of Protein Association. Productive diffusion-controlled protein−protein association by Brownian motion has been theoretically (*36*) and experimentally (*37*) shown to occur at 10^6−10^9 M^{-1} s^{-1}. The measured rate constant for association of wild-type Cdc25B with its protein substrate is in the expected range for proteins of this size. One might, therefore, expect mutations of hotspot residues to increase the apparent rate of dissociation, not decrease the apparent rate of association, because site-directed mutagenesis does not change the rate of free diffusion. In fact, there exists much precedence for hotspot mutations that produce faster dissociation rates (*4*, *38*−*42*). Thus, we were surprised to find that the hotspot mutations in both Cdc25B and its protein substrate exerted such a large effect on the rate of association. The unexpectedly large changes in the rate constants of association we observe, although rare, are not completely without precedence. For example, a $\sim$250-fold decrease in the association upon mutation of a single hotspot residue (K15A) in the interaction between trypsin and bovine pancreatic trypsin inhibitor has been observed (*43*). A $>$100-fold decrease in the association upon mutating hydrophobic residues (L17D and I31A) in the interaction between the Fc portion of human immunoglobulin G1 and a domain analogue of staphylococcal protein A has also been observed (*26*). Additionally, multiple simultaneous mutations in the TEM1 and BLIP protein complex have also led to dramatic changes ($>$100-fold) in the apparent rates of association (*6*).

The interaction between the Cdc25B and Cdk2-pTpY/CycA proteins is for purposes of forming a transient E·S complex, in contrast to the tighter protein−protein interactions previously characterized to such an extent. It may indeed be more advantageous for an E·S system to possess a remote binding site facilitating association rather than preventing dissociation. Increasing the stability through slow dissociation of E·S at a remote binding site that remains unchanged during catalysis would be counterproductive because this would also yield a tight-binding product complex. Similar considerations have been applied to the interpretation of hotspot mutants of Ras with its effectors wherein readily reversible complex formation is also important for biological function (*44*).

A possible physical mechanism that can account for the drastically reduced rate constants for association that we observe for the hotspot mutants is electrostatic enhancement. As pioneered by Schreiber and Fersht, the contribution of somewhat nonspecific Coulombic interactions can be several orders of magnitude (*45*, *46*). The basic concept is that long-range steering forces generated by patches of oppositely charged residues on the surface of each protein assist the association process by imposing directionality to the random collision process (*47*). Given that some of our hotspot residues are charged (Arg488, Arg492, and Asp206), one can easily imagine that they play a pivotal role in creating complementary electrostatic fields, thereby driving enzyme−substrate association via such electrostatic steering forces. This scenario is compatible with one-step association (Scheme 1) with which we have interpreted all our data. Unfortunately, we have been unable to test the role of electrostatic contributions directly because of the sensitivity of Cdc25B, like many other cysteine phosphatases (*48*), to inhibition by high ionic strength, even when using small molecule substrates (data not shown). Alternatively, a two-step model could account for the apparently slowed rate constants for association, but at present, there is no evidence to support such a model.

Remote docking sites such as the one we have characterized here for Cdc25B have been implicated in promoting specificity and/or catalysis for numerous protein kinases and phosphatases. Most well-known is the common docking (CD) site used by the MAP kinases for the binding of protein substrates, a site that is also used by the MAP kinase phosphatases when MAP kinases serve as substrates (*49*). As for Cdc25B, Arg and Asp residues are also the most critical residues in the CD site, although detailed kinetic studies have not yet elucidated the individual contributions

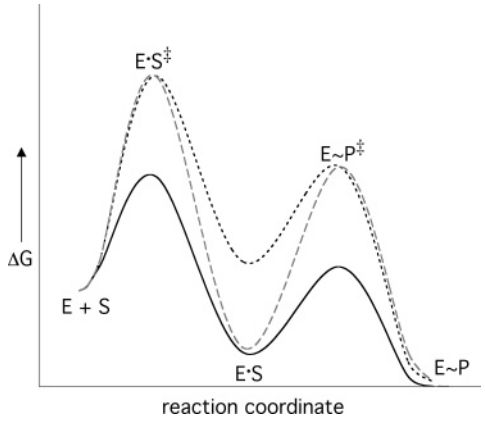

FIGURE 9: Working model for the Gibbs free energy diagram of the first half-reaction catalyzed by Cdc25B and its hotspot mutants. The first energy barrier represents the formation of the E·S complex, whereas the second barrier describes the chemical step that leads to the formation of the phospho-enzyme intermediate. The reaction for wild-type Cdc25B is denoted by a solid line. The reaction for mutants such as Arg488L is denoted by a dotted black line and for mutants such as R492L by a dashed gray line.

by residues in protein binding and subsequent catalysis. Our present studies provide a foundation and point of comparison for future investigations for the basis for transient protein−protein interactions such as these.

Hotspot Mutants and the Rate of Chemistry. Although the role of the remote hotspot residues in the formation of the E·S complex is intuitive, for a number of reasons, we were surprised to find significantly decreased rates of chemistry (k_2) for the mutants of Tyr497, Arg492, and Asp206, in particular the ~100-fold decrease for R492L (Table 1). First, the activities of hotspot mutants with small molecule substrates that probe both the formation and subsequent hydrolysis of the phospho-enzyme intermediate were unchanged (*15*, *16*). Second, the structure of R492L shows only minor perturbations in the region of the mutation and no changes in the active site region (Figure 4). Third, the R492K and R492A mutants showed smaller or no changes in k_2, respectively. Our current interpretation of these kinetic results is best visualized using a reaction coordinate diagram (Figure 9). For mutants with unchanged rates of chemistry (e.g., R488L), the E·S complex and the subsequent transition to product exist at equally raised energy levels compared to the raised transition state for E·S formation. For such mutants, the barriers between E·S and the transition states in either direction, as reflected in k_{off} and k_2, remain unchanged. In contrast, a slower k_2 for R492L can be explained by an unusual stabilization of the E·S complex. This model predicts a slowed rate constant for dissociation for the R492L mutant compared to that of the wild-type enzyme. Although untested, this hypothesis is consistent with the correlation between k_{on} and k_{cat}/K_m, which requires that k_{off} for R492L is significantly slower than the greatly reduced k_2 for R492L and thereby must be significantly slower than the estimated k_{off} for the wild-type enzyme. The molecular interactions between R492L and Cdk2-pTpY/CycA that facilitate such a stabilized E·S complex are unknown. Also it is unclear why and how such a nonproductive complex forms with R492L but not with R492A. We note that misalignment of just fractions of 1 Å at the active site can lead to greatly slowed reaction rates for nucleophilic attacks, thus making a full analysis even with high-resolution crystal structures difficult.

Catalytic Cycle with Protein Substrate. The kinetic mechanism for Cdc25B activity with the protein substrate was developed on the basis of the general scheme developed for PTPs reacting with small molecule substrates (Scheme 1) (*50*). Given the large discrepancy in activity between small molecule substrates and the protein substrate, it is theoretically possible that Cdc25B uses a completely different catalytic strategy with the protein substrate. Additionally, unlike activity with small molecule substrates, the interaction between Cdc25B and its protein substrate consists of at least two distal points of contact, namely, the active site and the remote docking site (*15*, *16*). However, we have found that Cdc25B incorporates essentially the same overall catalytic mechanism for both small molecules and native protein substrates. Protein substrate recognition is rapid and is governed in large part by interactions at the remote docking site. Following the formation of the phospho-enzyme intermediate, the protein product must dissociate to allow access to water for the hydrolysis of this intermediate. The existence of the remote docking site suggests a significant affinity between the protein product and Cdc25B, regardless of the phosphorylation status at the active site and potentially challenges the hypothesis of prompt product dissociation. However, we believe our comparative binding and kinetic studies with the wild-type enzyme and its active site mutants demonstrate that Cdc25B is exquisitely sensitive to the phosphorylation status of the protein substrate. Thus, following the formation of the phospho-enzyme intermediate, the loss of binding at the active site promotes the dissociation of the protein product, re-opening the active site for an incoming water molecule and the subsequent hydrolysis of the phospho-enzyme intermediate.

ACKNOWLEDGMENT

We thank the reviewers for their careful reading, thorough analysis, and insightful comments on this article.

REFERENCES

1. Clackson, T., and Wells, J. A. (1995) A hot spot of binding energy in a hormone-receptor interface, *Science 267*, 383−386.
2. Bogan, A. A., and Thorn, K. S. (1998) Anatomy of hot spots in protein interfaces, *J. Mol. Biol. 280*, 1−9.
3. Li, Y., Lipschultz, C. A., Mohan, S., and Smith-Gill, S. J. (2001) Mutations of an epitope hot-spot reside alter rate limiting steps of antigen-antibody protein-protein associations, *Biochemistry 40*, 2011−2022.
4. Wu, L. C., Tuot, D. S., Lyons, D. S., Garcia, K. C., and Davis, M. M. (2002) Two-step binding mechanism for T-cell receptor recognition of peptide-MHC, *Nature 418*, 552−556.
5. Vijayakumar, M., Wong, K.-Y., Schreiber, G., Fersht, A. R., Szabo, A., and Zhou, H.-X. (1998) Electrostatic enhancement of diffusion-controlled protein-protein association: Comparison of theory and experiment on barnase and barstar, *J. Mol. Biol. 278*, 1015−1024.
6. Selzer, T., and Schreiber, G. (2001) New insights into the mechanism of protein-protein association, *Proteins 45*, 190−198.
7. Hoffmann, I., and Karsenti, E. (1994) The role of cdc25 in checkpoints and feedback controls in the eukaryotic cell cycle, *J. Cell Sci. S18*, 75−79.
8. Nilsson, I., and Hoffmann, I. (2000) Cell cycle regulation by the Cdc25 phosphatase family, *Prog. Cell Cycle Res. 4*, 107−114.
9. Kristjánsdóttir, K., and Rudolph, J. (2004) Cdc25 phosphatases and cancer, *Chem. Biol. 11*, 1043−1051.
10. Iliakis, G., Wang, Y., Guan, J., and Wang, H. (2003) DNA damage checkpoint control in cells exposed to ionizing radiation, *Oncogene 22*, 5834−5847.

11. Jackson, M. D., and Denu, J. M. (2001) Molecular reactions of protein phosphatases: Insights from structure and chemistry, *Chem. Rev. 101*, 2313−2340.
12. Fauman, E. B., Cogswell, J. P., Lovejoy, B., Rocque, W. J., Holmes, W., Montana, V. G., Piwnica-Worms, H., Rink, M. J., and Saper, M. A. (1998) Crystal structure of the catalytic domain of the human cell cycle control phosphatase, Cdc25A, *Cell 93*, 617−625.
13. Reynolds, R. A., Yem, A. W., Wolfe, C. L., Deibel, M. R. J., Chidester, C. G., and Watenpaugh, K. D. (1999) Crystal structure of the catalytic subunit of Cdc25B required for G2/M phase transition of the cell cycle, *J. Mol. Biol. 293*, 559−568.
14. Rudolph, J., Epstein, D. M., Parker, L., and Eckstein, J. (2001) Specificity of natural and artificial substrates for human Cdc25A, *Anal. Biochem. 289*, 43−51.
15. Sohn, J., Kristjánsdóttir, K., Safi, A., Parker, B., Kiburz, B., and Rudolph, J. (2004) Remote hotspots mediate protein substrate recognition for the Cdc25 phosphatase, *Proc. Natl. Acad. Sci. U.S.A. 47*, 16437−16441.
16. Sohn, J., Parks, J. M., Buhrman, G., Brown, P., Kristjansdottir, K., Safi, A., Edelsbrunner, H., Yang, W., and Rudolph, J. (2005) Experimental validation of the docking orientation of Cdc25 with its Cdk2/CycA protein substrate, *Biochemistry 44*, 16563−16573.
17. Gottlin, E., Epstein, D. M., Eckstein, J., and Dixon, J. (1996) Kinetic analysis of the catalytic domain of human Cdc25B, *J. Biol. Chem. 272*, 27445−27449.
18. Chen, W., Wilborn, M., and Rudolph, J. (2000) Dual-specific Cdc25B phosphatase: in search of the catalytic acid, *Biochemistry 39*, 10781−10789.
19. McCain, D. F., Catrina, I. E., Hengge, A. C., and Zhang, Z.-Y. (2002) The catalytic mechanism of Cdc25A phosphatase, *J. Biol. Chem. 277*, 11190−11200.
20. McCain, D. F., Grzyska, P. K., Wu, L., Hengge, A. C., and Zhang, Z.-Y. (2004) Mechanistic studies of protein tyrosine phosphatases YopH and Cdc25A with m-nitrobenzyl phosphate, *Biochem. 43*, 8256−8264.
21. Johnson, K. (1992) Transient-state kinetic analysis of enzyme reaction pathways, *The Enzymes XX*, 1−61.
22. Buhrman, G., Parker, B., Sohn, J., Rudolph, J., and Mattos, C. (2005) Structural mechanism of oxidative regulation of the phosphatase Cdc25B via an intramolecular disulfide bond, *Biochemistry 44*, 5307−5316.
23. Jeffrey, P. D., Russo, A. A., Polyak, K., Gibbs, E., Hurwitz, J., Massagué, J., and Pavletich, N. P. (1995) Mechanism of CDK activation revealed by the structure of a CyclinA-CDK2 complex, *Nature 376*, 313−320.
24. Kristjánsdóttir, K., and Rudolph, J. (2003) A fluorescence polarization assay for native protein substrates of kinases, *Anal. Biochem. 316*, 41−49.
25. Schreiber, G., and Fersht, A. R. (1993) Interaction of barnase with its polypeptide inhibitor barstar studied by protein engineering, *Biochemistry 18*, 5145−5150.
26. Jendeberg, L., Persson, B., Andersson, R., Karlsson, R., Uhlen, M., and Nilsson, B. (1995) Kinetic analysis of the interaction between protein A domain variants and human Fc using plasmon resonance detection, *J. Mol. Recognit. 8*, 270−278.
27. Sydor, J. R., Engelhard, M., Wittinghofer, A., Goody, R. S., and Herrmann, C. (1998) Transient kinetic studies on the interaction of Ras and the Ras-binding domain of c-Raf-1 reveal rapid equilibration of the complex, *Biochemistry 37*, 14292−14299.
28. Beebe, J. A., and Fierke, C. A. (1994) A kinetic mechanism for cleavage of precursor tRNA(Asp) catalyzed by the RNA component of Bacillus subtilis ribonuclease P, *Biochemistry 33*, 10294−10304.
29. Fierke, C. A., and Hammes, G. G. (1995) Transient kinetic approaches to enzyme mechanisms, *Methods Enzymol. 249*, 3−37.
30. Wilborn, M., Free, S., Ban, A., and Rudolph, J. (2001) The C-terminal tail of the dual-specificity Cdc25B phosphatase mediates modular substrate recognition, *Biochemistry 40*, 14200−14206.
31. Xu, X., and Burke, S. P. (1996) Roles of active site residues and the NH2-terminal domain in the catalysis and substrate binding of human Cdc25, *J. Biol. Chem. 271*, 5118−5124.
32. Morrison, J. F. (1969) Kinetics of the reversible inhibition of enzyme-catalysed reactions by tight-binding inhibitors, *Biochem. Biophys. Acta 185*, 269−286.
33. Cheng, Y.-C., and Prusoff, W. H. (1972) Relationship between the inhibition constant (Ki) and the concentration of inhibitor which causes 50 percent inhibition (IC50) of an enzymatic reaction, *Biochem. Pharmacol. 22*, 3099−3108.
34. Sullivan, J. E., Holdgate, G. A., Campbell, D., Timms, D., Gerhardt, S., Breed, J., Breeze, A. L., Bermingham, A., Paupit, R. A., Norman, R. A., Embrey, K. J., Read, J., VanScyoc, W. S., and Ward, W. H. J. (2005) Prevention of MKK6-dependent activation by binding to p38alpha MAP kinase, *Biochemistry 44*, 16475−16490.
35. Sohn, J., and Rudolph, J. (2006) The energetic network of hotspot residues between Cdc25B phosphatase and its protein substrate, *J. Mol. Biol. 362*, 1060−1071.
36. Northrup, S. H., and Erickson, H. P. (1992) Kinetics of protein-protein association explained by Brownian dynamics computer simulation, *Proc. Natl. Acad. Sci. U.S.A. 89*, 3338−3342.
37. Koren, R., and Hammes, G. G. (1976) A kinetic study of protein-protein interactions, *Biochemistry 15*, 1165−1171.
38. Schreiber, S., and Fersht, A. R. (1995) Energetics of protein-protein interactions: analysis of the barnase-barstar interface by single mutations and double mutant cycles, *J. Mol. Biol. 248*, 478−486.
39. Albeck, S., Unger, R., and Schreiber, G. (2000) Evaluation of direct and cooperative contributions towards the strength of buried hydrogen bonds and salt bridges, *J. Mol. Biol. 298*, 503−520.
40. Camacho, C. J., Kimura, S. R., DeLisi, C., and Vajda, S. (2000) Kinetics of desolvation-mediated protein-protein binding, *Biophys. J. 78*, 1094−1105.
41. Sinha, N., Mohan, S., Lipschultz, C. A., and Smith-Gill, S. J. (2002) Differences in electrostatic properties at antibody-antigen binding sites: implications for specificity and cross-reactivity, *Biophys. J. 83*, 2946−2968.
42. Rajamani, D., Thiel, S., Vajda, S., and Camacho, C. J. (2004) Anchor residues in protein-protein interactions, *Proc. Natl. Acad. Sci. U.S.A. 101*, 11287−11292.
43. Castro, M. J. M., and Anderson, S. (1996) Alanine point-mutations in the reactive region of bovine pancreatic trypsin inhibitor: effects on the kinetics and thermodynamics of binding to β-trypsin and α-chymotrypsin, *Biochemistry 35*, 11435−11446.
44. Kiel, C., Serrano, L., and Herrmann, C. (2004) A detailed thermodynamic analysis of Ras/Effector complex interfaces, *J. Mol. Biol. 340*, 1039−1058.
45. Schreiber, G., and Fersht, A. R. (1996) Rapid, electrostatically assisted association of proteins, *Nat. Struct. Biol. 3*, 427−431.
46. Selzer, T., and Schreiber, G. (1999) Predicting the rate enhancement of protein complex formation from the electrostatic energy of interaction, *J. Mol. Biol. 287*, 409−419.
47. Janin, J. (1997) The kinetics of protein-protein recognition, *Proteins 28*, 153−161.
48. Niu, T., Liang, X., Yang, J., Zhao, Z. J., and Zhou, G. W. (1999) Kinetic comparison of the catalytic domains of SHP-1 and SHP-2, *J. Cell. Biochem. 72*, 145−150.
49. Tanoue, T., and Nishida, E. (2003) Molecular recognitions in the MAP kinase cascades, *Cell. Signalling 15*, 455−462.
50. Denu, J. M., and Dixon, J. E. (1995) A catalytic mechanism for the dual-specific phosphatases, *Proc. Natl. Acad. Sci. U.S.A. 92*, 5910−5914.

BI061257Y